Journal of Nano- and Electronic Physics
Vol. **10** No 3, 03001(6pp) (2018)

Журнал нано- та електронної фізики
Том **10** № 3, 03001(6cc) (2018)

High Band Gap Nanocrystalline Tungsten Carbide (nc-WC) Thin Films Grown by Hot Wire Chemical Vapor Deposition (HW-CVD) Method

Bharat Gabhale[1], Ashok Jadhawar[1], Ajinkya Bhorde[1], Shruthi Nair[1], Haribhau Borate[1], Ravindra Waykar[1], Rahul Aher[1], Priyanka Sharma[1], Amit Pawbake[1*], Sandesh Jadkar[2*]

[1] *School of Energy Studies, Savitribai Phule Pune University, 411 007 Pune, India*
[2] *Department of Physics, Savitribai Phule Pune University, 411 007 Pune, India*

(Received 01 March 2018; revised manuscript received 09 June 2018; published online 25 June 2018)

In present study nanocrystalline tungsten carbide (nc-WC) thin films were deposited by HW-CVD using heated W filament and CF_4 gas. Influence of CF_4 flow rate on structural, optical and electrical properties has been investigated. Formation of WC thin films was confirmed by low angle XRD, Raman spectroscopy and x-ray photoelectron spectroscopy (XPS) analysis. Low angle XRD analysis revealed that WC crystallites have preferred orientation in (101) direction and with increase in CF_4 flow rate the volume fraction of WC crystallites and its average grain size increases. Formation of nano-sized WC was also confirmed by transmission electron microscopy (TEM) analysis. UV-Visible spectroscopy analysis revealed increase in optical transmission with increase in CF_4 flow rate. The WC film deposited for 40 sccm of CF_4 flow rate show high transparency (~ 80-85 %) ranging from visible to infrared wavelengths region. The band gap shows increasing trend with increase in CF_4 flow rate (3.48-4.18 eV). The electrical conductivity measured using Hall Effect was found in the range ~ 103-141 S/cm over the entire range of CF_4 flow rate studied. The obtained results suggest that these wide band gap and conducting nc-WC films can be used as low cost counter electrodes in DSSCs and co-catalyst in electrochemical water splitting for hydrogen production.

Keywords: WC films, HW-CVD, Low angle XRD, Raman spectroscopy, XPS.

DOI: 10.21272/jnep.10(3).03001 PACS numbers: 81.15.Cd, 81.07.Bc

1. INTRODUCTION

Sustainable hydrogen production through electrosplitting of water and improvement in conversion efficiency of dye-sensitized solar cells (DSSCs) has attracted great scientific interest in the past two decades. The conventional noble metal based electro-catalysts such as Pt have very limited use in the electrolysis of water due to their high cost and scarcity [1]. An attempt has been made to use several non-noble-metal materials such as transition-metal chalcogenides [2], carbides [3], and metal alloys [4] as catalysts for application in the hydrogen evolving reaction. In DSSC, FTO glass loaded with Pt as a conventional counter electrode with good electro-catalytic properties employed for the reduction of tri-iodide to iodide. Finding low cost substitutes for Pt as an alternative counter electrode in the DSSC is therefore essential. Several new materials, such as carbon materials and organic polymers, have been proposed to replace Pt [5]. But, these materials have low catalytic activity, bad corrosion resistance to a corrosive redox couple in electrolyte and poor thermal stability.

Tungsten carbide (WC) finds potential applications owing to its unusual properties, such as high melting point, superior hardness, low friction coefficient, high oxidation resistance, and superior electrical conductivity [6]. The material has been successfully employed hydrogen evolution reaction (HER) [7], lithium ion batteries and counter electrode in dye synthesised solar cell [8] and effective catalyst for methanol electro-oxidization and oxygen reduction reaction [9, 10]. Recently, Cui et.al [11] used WC as an efficient anode buffer layer for a high-performance inverted organic solar cell and achieved conversion efficiency 8.04 %. The Pt-like performance of WC as catalyst and Pt can be partially or totally replace by it [12] due to the low cost, high catalytic activity, selectivity, and good thermal stability under rigorous conditions. Furthermore, WC has higher resistance in acidic solution and higher temperature. It showed a resistance to the CO poisoning, leading to prolonged catalytic life for direct alcohol fuel cells. There are several methods used for the preparation of WC powder, including the direct carburization of tungsten powder, solid-state metathesis, reduction carburization, mechanical milling, and polymeric precursor routes using metal alkoxides. Traditionally the production of WC involves two steps. First, the oxide is reduced to high-purity tungsten in a hydrogen atmosphere. The tungsten metal is then mixed with the required amount of carbon and reacts at a temperature of 1400-1600 ^{0}C to produce WC [13]. However, these methods have several disadvantages such as complex procedures, long time, high temperatures and high energy consumption. Most importantly, the resultant WC particles are generally big in size and lower in specific surface area. Furthermore it is hardly to obtain pure WC. To prepare WC nanoparticles with cost efficient method, lower energy expenditure, and controllable particle size is a critical challenge for wide application of WC in industries. The WC coatings can be deposited by various deposition techniques which includes plasma spraying [14] chemical vapor deposition [15], physical vapor deposition [7], DC magnetron sputtering [8], simultaneous RF sputtering [9], spray paste [10], plasma enhanced chemical va-

*sandesh@physics.unipune.ac.in
tamitpawbake@gmail.com

por deposition (PE-CVD) [16], plasma-assisted atomic layer deposition [17] etc. Each method has its advantages and limitations. Among these methods the HW-CVD has emerged as a promising technique to deposit Si based thin films such as a-Si:H, μc/nc-Si:H, poly-Si, SiGe and SiC alloys, SiN_x etc. To our knowledge, this method has not been fully studied for the synthesis of WC films and there exist few reports in the literature [18]. With this motivation an attempt has been made to prepare WC films using HW-CVD method.

Herein, we report the deposition of nanocrystalline WC thin films by HW-CVD simply passing Tetra-fluoromethane (CF_4) gas over the heated W filament. The influence of CF_4 flow rate on structural, optical and electrical properties has been investigated. The films were analyzed by variety of techniques such as low angle XRD, Raman spectroscopy, x-ray photoelectron spectroscopy (XPS), transmission electron microscopy (TEM), UV-Visible-IR spectroscopy and Hall Effect measurements. It has been observed that properties of WC thin films critically depend on CF_4 flow rate.

2. EXPERIMENTAL

2.1 Preparation of Films

The WC thin films were deposited simultaneously on Corning #7059 glass and c-Si wafers in a locally fabricated HW-CVD system, details of which have been described elsewhere [19] using heated tungsten (W) filament (Goodfellow, Sigma Aldrich) and pure Tetra-fluoro-methane (CF_4) gas (VLSI grade) as C source gas. The flow rate of CF_4 was varied between 10 sccm to 40 sccm in the step of 10 sccm. The filament temperature was kept constant at 1900 °C and was measured by optical pyrometer (IRCON, USA). The pressure during deposition was kept constant at 50 ± 5 mTorr using manual throttle valve. The substrate temperature was held constant (350 °C) using a thermocouple and temperature controller and filament-to-substrate distance ($d_{s\text{-}f}$) was fixed at 5 cm. Other deposition parameters are listed in Table 1.

Table 1 – Process parameters employed during the deposition of WC films by HW-CVD method

Process parameter	Value
Deposition pressure (P_d)	50 mTorr
Deposition time (t)	25 min
Filament temperature (T_{fil})	1900 °C
Filament to substrate distance ($d_{s\text{-}f}$)	5 cm
CF_4 gas flow rate (F_{CF4})	10-40 sccm
Substrate temperature (T_{sub})	350 °C

The glass substrates were cleaned with double distilled water whereas, the c-Si wafers were etched using solution of HF to remove native oxide layer. The substrates were loaded to the substrate holder and then the deposition chamber was evacuated to the base pressure less than 10^{-6} Torr. Prior to each deposition, the substrate holder and deposition chamber were baked for two hours at 100 °C to remove any water vapor absorbed on the substrates and to reduce the oxygen contamination in the film. After that, the substrate temperature was brought to desired value by appropriately setting the inbuilt thermocouple and temperature controller. The deposition was carried out for desired amount of time and films were allowed to cool to room temperature in vacuum.

2.2 Characterization of Films

Electrical conductivity was measured by using Van der Paw method (Ecopia HMS-3000 Hall Measurement System) at room temperature. Optical band gap was deduced from transmittance and reflectance spectra of the films deposited on corning glass using a JASCO, V-670 UV-Visible-Infrared spectrophotometer in the range 250-2500 nm by using the procedure followed by Tauc. Raman spectra were recorded with Raman spectroscopy instrument (Renishaw inVia confocal Raman microscope) in the range 600-2100 cm^{-1}. The spectrometer has backscattering geometry for detection of Raman spectrum with the resolution of 1 cm^{-1}. The excitation source was 532 nm line of He-Ne laser. The power of the Raman laser was kept to less than 5 mW to avoid laser induced crystallization on the films. Low angle x-ray diffraction pattern were obtained by x-ray diffractometer (Bruker D8 Advance, Germany) using Cu K_α line (λ = 1.54056 Å). The patterns were taken at a grazing angle of 1°. The average crystallite size was estimated using the classical Scherrer's formula,

$$d_{x\text{-}ray} = \frac{0.9\ \lambda}{\beta \cos\theta_B}, \qquad (1)$$

where, λ is the wavelength of diffracted radiation, θ_B is the Bragg angle and β FWHM in radians. The XPS studies were carried out using VSW ESCA machine, under the vacuum of better than $> 10^{-9}$ Torr, with AlK_α (1486.6 eV) radiation with resolution of 0.1 eV. The XPS signal was obtained after several scans in the acquisition process. The spectra were recorded for all the elements as well as for specific elements. Transmission electron microscopy (TEM) images and selected area electron diffraction (SAED) pattern were recorded using a transmission electron microscope (TECNAI G^2 – 20-TWIN, FEI, The Netherlands) operating at 200 keV. Thickness of films was determined by profilometer (KLA Tencor, P-16+).

3. RESULTS AND DISCUSSION

In the present study, W wire (filament) is heated at high temperature (~ 1900 °C) in the controlled CF_4 atmosphere. We think that there are two possibilities for the growth of WC thin films. First, due to high temperature W can be evaporated and travel towards the heated substrate in presence of CF_4. Before reaching the substrate surface, the radical and gas-phase reactions may takes place which leads to the formation of WC thin film at the substrate surface. Second, at elevated temperatures (red heat), the WC is formed at the filament. These WC may boiled off from the filament get deposited at substrate surface.

3.1 Variation in Deposition Rate

Films were deposited for a desired time period (25 min) and deposition rate is then calculated from

thickness measurement. The variation of deposition rate as a function of CF_4 flow rate is shown in figure 1. As seen from the figure the deposition rate decreases from 29.6 nm/min to 12.6 nm/min when CF_4 flow rate increase from 10 sccm to 40 sccm.

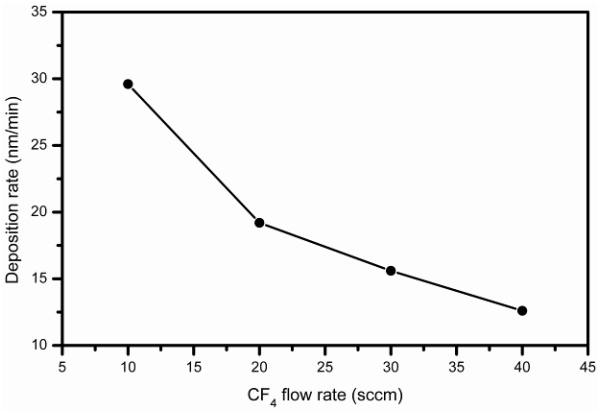

Fig. 1 – Variation of deposition rate as a function of CF_4 flow rate for WC films deposited by HW-CVD method

In HW-CVD decrease in deposition rate occurs due to etching effect of atomic H. In the present study no hydrogen dilution of CF_4 is used. Hence the etching of growing surface due to atomic H is ruled out. We believe that the deposition rate is filament temperature dependent reaction rate taking place at the filament surface and/or radical-radical reactions occurring in the vicinity of substrate surface. At low CF_4 flow rates due to complete decomposition of CH_4 at the heated filament the supply of WC film forming species are large. As a result the deposition rate is high when the WC films are deposited at low CF_4 flow rate. However, with increase in CF_4 flow rate the supply of film forming species may be limited by incomplete decomposition of CF_4 at the heated filament as well as possibility of formation of low sticking coefficient species due to radical-radical reactions occurring in the process chamber near the substrate surface. As a result deposition rate is low for WC films deposited at high CF_4 flow rates.

3.2 Low Angle XRD Analysis

Low angle x-ray diffraction (low angle-XRD) is a widely used non-destructive technique for the structural characterization of different materials. Figure 2 shows low angle-XRD pattern of as-deposited WC thin films deposited on glass substrate at various CF_4 flow rates. All low angle-XRD patterns were obtained at a grazing angle of 1°. Presence of multiple diffraction peaks indicates the polycrystalline nature of thin films. As seen from the XRD pattern the film deposited at low CF_4 flow rate (10 sccm) shows diffraction peaks at $2\theta \sim 48.5°$, 62.9° and 70.0° corresponding to (101), (110) and (111) diffraction planes, respectively, which are characteristic of hexagonal structure of WC [20]. In addition, two other diffraction peaks were also observed in the diffraction pattern at $2\theta \sim 43.4°$ associated with WC_{1-x} structure [12] and other broad diffraction peak centered at $2\theta \sim$ 24-25° corresponds to amorphous carbon (a-C) implying a non-graphitized carbon structure [21]. With increase in CF_4 flow rate the diffraction peak corresponding to a-C disappears and two distinct peaks at $2\theta \sim 23.3°$ and 24.5° associated with WC were observed with preferred orientation along (101) direction. With increase in CF_4 flow rate the full width at half maximum (FWHM) of (101) diffraction plane decreases whereas its intensity increases. These results indicate increase in volume fraction of WC crystallites and its size (6-10 nm).

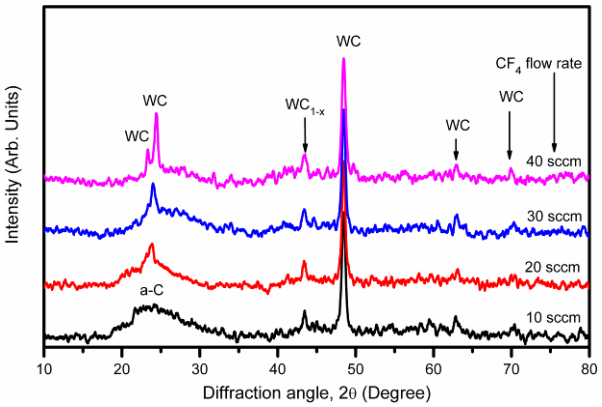

Fig. 2 – Low angle-XRD pattern of WC thin films deposited on glass substrate at various CF_4 flow rates

No other diffraction peaks due to various allotropes of tungsten carbide were found suggesting formation of pure phase nano-sized tungsten carbide thin films by using HW-CVD method.

3.3 Raman Spectroscopy Analysis

Raman spectroscopy is a very powerful non-destructive technique used to investigate the structure of materials because it gives a fast and simple way to determine the phase of the material, whether it is amorphous, crystalline or nanocrystalline. Formation of tungsten carbide thin films was further confirmed by Raman spectroscopy. Figure 3 shows the Raman spectra of WC films deposited at different CF_4 flow rates by using HW-CVD method. As seen from the Raman spectra films deposited at various CF_4 flow rates shows peaks at $\sim 709\ cm^{-1}$ and $806\ cm^{-1}$ corresponding to WC [22] thin films.

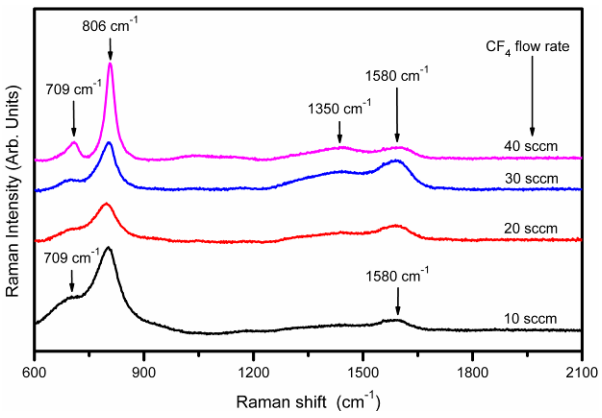

Fig. 3 – Raman spectra of WC films deposited at different CF_4 flow rates

These results further confirm the formation of WC

films by HW-CVD method. In addition, two broad shoulders were observed in the Raman spectra for the WC films deposited at various CF_4 flow rates, one at ~ 1350 cm^{-1} and another at ~ 1580 cm^{-1} corresponding to D and G bands respectively [23]. The D band represent defects which are might be due to dislocations, missing atoms at the edges of the sample and *sp*3-hybridized carbon atoms.

3.4 Transmission Electron Microscopy (TEM) Analysis

Further to confirm the formation of nanocrystalline WC films, transmission electron microscopy (TEM) analysis was performed. Figure 4(a) shows the bright TEM image of WC film synthesized for 40 sccm of CF_4 flow rate. It clearly shows the formation of WC crystallites having average crystallite size ~ 10-12 nm. These results are consistent with low angle XRD analysis. Figure 4(b) shows the high resolution TEM image of WC film for same CF_4 flow rate. The insert of figure 4(b) is selected area electron diffraction (SAED) pattern of WC film synthesized for 40 sccm of CF_4 flow rate.

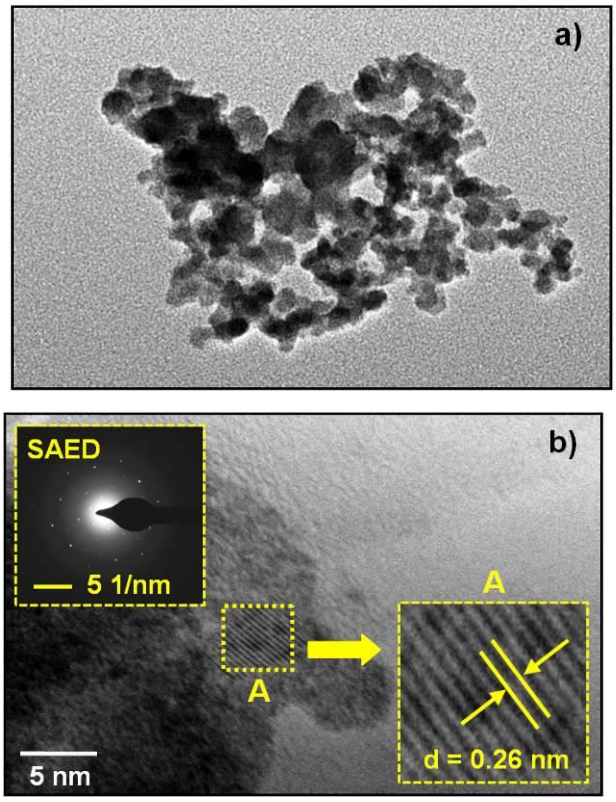

Fig. 4 – Transmission electron microscopy (TEM) analysis of WC film synthesized for 40 sccm of CF_4 flow rate a) Bright TEM image b) High resolution TEM (HR-TEM) image. The insert (top left corner) is selected area electron diffraction (SAED) pattern. The bottom right corner in the inset is the enlarged view of area 'A' of HR-TEM image

The bright spots in the SAED pattern signify polycrystalline structure and a high degree of crystallinity of WC film. These results are also consistent with XRD analysis. In the inset figure 4(b) is the enlarged view of area 'A' of WC film synthesized for 40 sccm of CF_4 flow rate. It is evident from the that the distance between the adjacent lattice planes is ~ 0.26 nm, which were well in agree those reported in the literature [24]. These results further confirm the formation of nano-sized tungsten carbide thin films by using HW-CVD method.

3.5 X-ray Photoelectron Spectroscopy (XPS) Analysis

The composition and atomic bonding states in WC films have been performed by using x-ray photoelectron spectroscopy (XPS). Figure 5 shows the XPS survey scan of HW-CVD deposited tungsten carbide film at 40 sccm CF_4 flow rate. The scan shows the tungsten [W(4*f*), W(4*d*), W(4*p*) and W(4*s*)], carbon [(C(1*s*)], oxygen [O(1*s*)] peaks. These peaks are consistent with the XPS spectra of W containing a-C films deposited by pulsed vacuum arc method by Monteiro et al. [25].

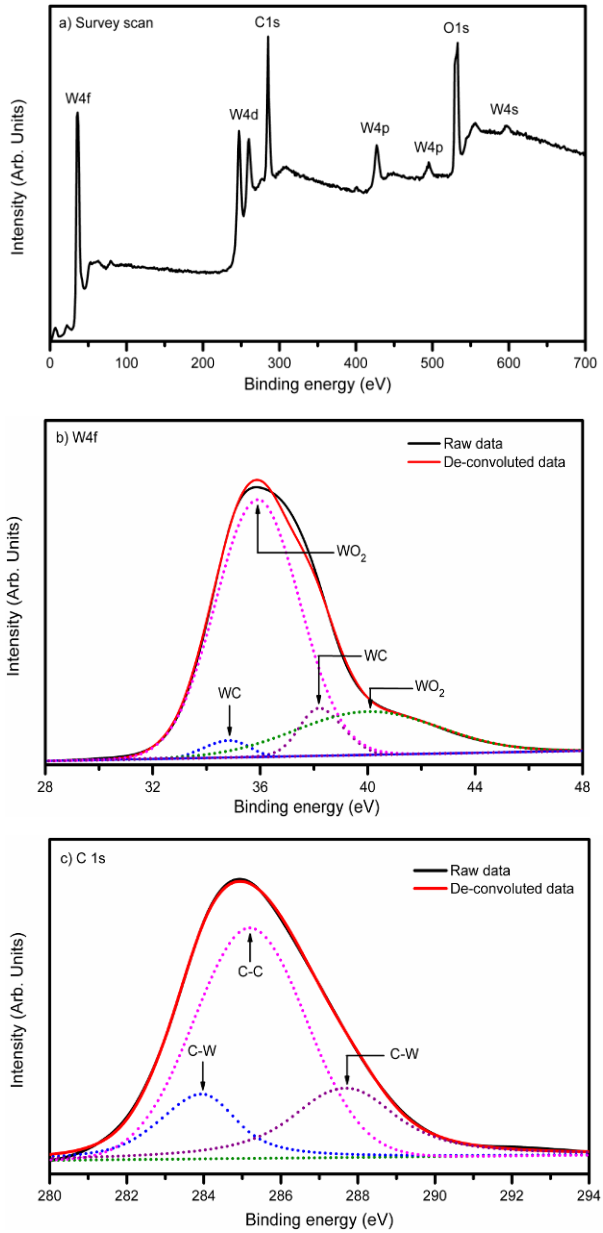

Fig. 5 – Typical XPS spectra for WC film deposited at 40 sccm CF_4 flow rate by HW-CVD method (a) Survey scan in the range 0-700 eV (b) de-convoluted XPS spectra of W (4*f*) in the range 28-48 eV (c) de-convoluted XPS spectra of C 2*s* peak in

the range 279-295 eV

The oxygen peak is originated due to adsorbed oxygen and surface oxidation of the film. The oxygen was found to be incorporated in films prepared at even lower base pressure than the pressure employed for the XPS measurements [26]. The measured XPS spectrum is a superposition of peaks from the various types of bonds, and therefore it is necessary to de-convolute the survey spectra to determine the chemical bond configurations present in the sample. The spectra could be decomposed into several peaks based on the assumption that each peak consists of the Gaussian/Lorentz sum function [26]. Figures 5(b) and 5(c) show typical de-convoluted XPS spectra of W (4*f*) and C (1s) electron state, respectively. The W (4f) spectra (28-48 eV) exhibit four different peaks at binding energies ~ 40.12 eV, ~ 38.18 eV, ~ 35.90 eV and ~ 34.83 eV, which were assigned to the $5p^{3/2}$ of WO_2, $5p^{3/2}$ of WC, $4f^{5/2}$ of WO_2, $4f^{5/2}$ of tungsten carbide [25]. No signal corresponding to metallic W has been observed indicating that W is present only as carbide and oxide forms. The de-convoluted C (1s) spectra (280 eV – 294 eV) exhibit three different peaks at binding energies ~ 284.0 eV and ~ 285.18 eV associated with C-W bonding whereas the peak at binding energy ~ 287.75 eV assigned to C-C bonding [27]. The elemental mapping for the film deposited at 40 sccm CF_4 flow rate have been estimated and it is found that the film consist of 45 % of tungsten, 39 % of carbon and 16 % of oxygen.

3.6 UV-Visible Spectroscopy Analysis

Optical properties of WC thin films were investigated using UV-Visible spectroscopy. Optical transmission spectra of nanocrystalline WC deposited on substrate recorded in wavelength range 250-2500 nm is shown in figure 6(a). The transmission increases with increase in CF_4 flow rate and can be attributed to decrease in film thickness. Highest transmission (~ 80-85 %) in visible and infrared region has been observed for the WC film deposited at 40 sccm of CF_4 flow rate.

In the direct transition semiconductor, the optical energy band gap (E_{opt}) and the optical absorption coefficient (α) are related by,

$$(\alpha E)^{1/2} = B^{1/2}(E - E_{opt}), \qquad (2)$$

where α is the absorption coefficient, B is the optical density of state and E is the photon energy. The absorption coefficient (α) can be calculated from the transmittance of the films with the formula,

$$\alpha = \frac{1}{d} \ln\left(\frac{1}{T}\right), \qquad (3)$$

where d is the thickness of the films and T is the transmittance. Therefore, the optical band gap (E_{opt}) is obtained by extrapolating the tangential line to the photon energy ($E = h\upsilon$) axis in the plot of $(\alpha h\upsilon)^2$ as a function of $h\upsilon$ (Tauc plot). The optical band gaps of the films were determined from the extrapolation of the linear plot of $(\alpha h\upsilon)^{1/2}$ versus $h\upsilon$ at $\alpha = 0$ [see figure 6(b)]. The inset shows typical Tauc plot for WC film deposited at 40 sccm of CF_4 flow rate. The band gap values HW-CVD deposited WC films increases with increase in CF_4 flow rate. These values are higher than the tungsten carbide thin films obtained by simultaneous RF sputtering [9] and pulsed laser deposition technique at room temperature [28]. The increase in band gap can be attributed due to the increase in carbon content and increase in crystallinity in the film with increase in CF_4 flow rate. The low angle XRD analysis further supports this.

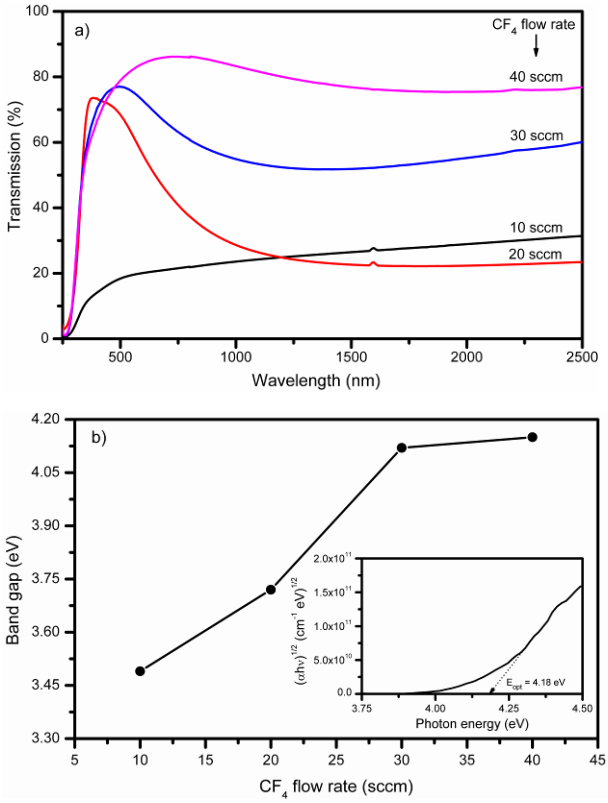

Fig. 6 – Transmittance spectra of WC films deposited at various CF_4 flow rates (a); variation of optical gap as a function of CF_4 flow rates for WC thin films deposited using HW-CVD method (b)

3.7 Electrical Properties

Hall Effect study is a powerful tool for knowing the electronic properties of thin film samples. Conductivity of WC films was measured using Van der Paw method (Ecopia HMS-3000 Hall Measurement System) at room temperature. For this four contacts were made by using indium wire at the four corners of the film sample of dimension 1 cm x 1 cm. The gold spring probes were placed at the corners of the sample symmetrically. *A* constant current of 1 nA was supplied to the films. The films were subjected to uniform magnetic field of 0.54 Tesla. A known current was passed through the electrodes of the films and voltage across the other two electrodes was measured. The polarity was reversed for each measurement and the voltage was measured. Figure 7 shows the variation of conductivity of WC films deposited at different CF_4 flow rates. As seen from the figure the conductivity gradually decreases from ~ 141.0 S/cm to ~ 103.46 S/cm when the CF_4 flow rate

increased from 10 sccm to 40 sccm. The error bars in the figure indicates differences in the measurement of conductivity of WC films due to change in contact points and due to change in polarity.

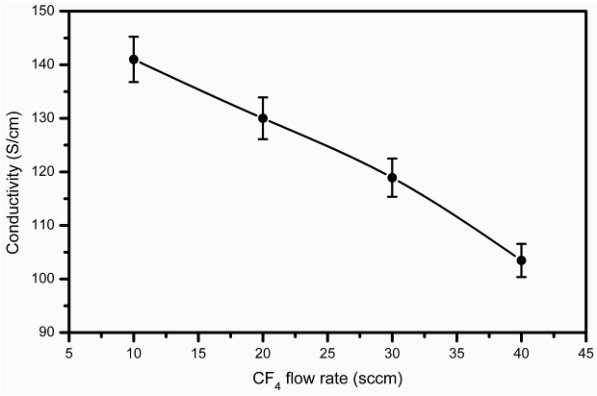

Fig. 7 – Variation of conductivity of WC films deposited at different CF_4 flow rates. The error bars indicates differences in the measurement of conductivity of WC films due to change in contact points and due to change in polarity

4. CONCULSION

In conclusion, thin films of tungsten carbide (WC) were grown successfully by HW-CVD using heated W filament and CF_4 gas. Influence of CF_4 flow rate on structural, optical and electrical properties has been investigated. The formation of WC thin films was confirmed by low angle XRD, Raman spectroscopy and x-ray photoelectron spectroscopy (XPS) analysis. The low angle XRD analysis revealed that WC crystallites have preferred orientation in (101) direction and with increase in CF_4 flow rate the volume fraction of WC crystallites and its average grain size increases. The formation of nano-sized WC was also confirmed by transmission electron microscopy (TEM) analysis. Optical properties were investigated using UV-Visible spectroscopy revealed increase in optical transmission with increase in CF_4 flow rate. The WC film deposited for 40 sccm of CF_4 flow rate showed good transparency (~ 80-85 %) ranging from visible to infrared wavelengths region. The band gap shows increasing trend with increase in CF_4 flow rate (3.48-4.18 eV). The electrical conductivity measured using Hall Effect was found in the range ~ 103-141 S/cm over the entire range of CF_4 flow rate studied. The obtained results suggest that such wide band gap and conducting tungsten carbide films can be used as low cost counter electrodes in DSSCs and co-catalyst in electrochemical water splitting for hydrogen production.

ACKNOWLEDGEMENT

Authors are thankful to Department of Science and Technology (DST), Ministry of New and Renewable Energy (MNRE), and University Grants Commission (UGC), Government of India, New Delhi for the financial support. One of the authors Sandesh Jadkar is thankful to University Grants Commission, New Delhi for special financial support under UPE program.

REFERENCES

1. J. Greeley, T.F. Jaramillo, J.Bonde, I. Chorkendorff, J.K. Norskov, *Nat. Mater.* **5**, 909 (2006).
2. T. Jaramillo, K. Jorgensen, J. Bonde, J. Nielsen, S. Horch, I. Chorkendorff, *Science* **317**, 100 (2007).
3. Y. Yan, L. Zhang, X. Qi, H. Song, J.Y. Wang, H. Zhang, X. Wang, *Small* **8**, 3350 (2012).
4. J.R. McKone, E.L. Warren, M.J. Bierman, S.W. Boettcher, B.S. Brunschwig, N.S. Lewis, H.B. Gray, *Energy Environ. Sci.* **4**, 3573 (2011).
5. E. Ramasamy, W. Lee, D. Lee, J. Song, *Electrochem. Commun.* **10**, 1087 (2008).
6. S. Shanmugam, D.S. Jacob, A. Gedanken, *J. Phys. Chem. B* **109**, 19056 (2005)
7. A. Czyzniewski, *Thin Solid Films* **433**, 180 (2003).
8. T. Tavsanoglu, C. Begum, M. Alkan, O. Yucel, *J. Min., Metals Mater. Soc. (JOM)* **65**, 562 (2013).
9. Y. Suda, K. Yukimura, K. Nakamura, K. Takaki, Y. Sakai, *Jpn. J. Appl. Phys.* **45**, 8449 (2006).
10. M. Wu, X. Lin, A. Hagfeldt, T. Ma, *Angew. Chem. Int. Ed.* **50**, 3520 (2011).
11. W. Cui, Z. Wu, C. Liu, M. Wu, T. Ma, S. Wang, S. Lee, B. Sun, *J. Mater. Chem. A* **2**, 3734 (2014).
12. Z. Yan, M. Cai, P. Shen, *Sci. Rep.* **3**, 1646 (2013).
13. J. M. Girandon, P. Devassine, J.F. Lamonier, L. Delannoy, L. Lecleveq, G. Leclereq, *J. Solid State Chem.* **154**, 412 (2000).
14. J. Guilemany, S. Dosta, J. Nin, J. Miguel, *J. Therm. Spray Techno.* **14/3**, 405 (2005).
15. J. Giraudon, P. Devassine, L. Leclercq, G. Leclercq, *J. Mater. Sci.* **33**, 1369 (1998).
16. H. Zheng, J. Huang, W. Wang, C. Ma, *Electrochem. Commu.* **7**, 1045 (2005).
17. D. Kim, Y. Kim, Y. Song, B. Lee, J. Kim, S. Suh, R. Gordon, *J. Electrochem. Soc.* **150**, C740 (2003).
18. A. Pawbake, R. Waykar, A. Jadhavar, R. Kulkarni, V. Waman, A. Date, D. Late, H. Pathan, S. Jadkar, *Mater. Lett.* **183** 315 (2016).
19. V. Waman, M. Kamble, M.R. Pramod, S. Gore, A. Funde, R. Hawaldar, D. Amalnerkar, V. Sathe, S. Gosavi, S. Jadkar, *J. Non- Cryst. Sol.* **357**, 3616 (2011).
20. A. Voevodin, J. O'Neill, S. Prasad, J. Zabinski, *J. Vac. Sci. Technol. A* **17**, 986 (1999).
21. X. Ma, L. Gan, M. Liu, P. Tripathi, Y. Zhao, Z. Xu, D. Zhu, L. Chen, *J. Mater. Chem. A* **2**, 8407 (2014).
22. Y. Yan, B. Xia, X. Qi, H. Wang, R. Xu, J. Wang, H. Zhang, X. Wang, *Chem. Commun.* **49**, 4884 (2013).
23. F. Withers, M. Dubois, A.K. Savchenko, *Phys. Rev. B* **82**, 073403 (2010).
24. M. Nie, P. Shen, Z. Wei, Q. Li, H. Bi, C. Liang, *ECS Electrochem. Lett.* **1/3**, H11 (2012).
25. O. Monteiro, M. Ogletree, I.G. Brown, *Thin Solid Films* **342**, 100 (1999).
26. T. Wu, H. Shen, B. Cheng, Y. Pan, B. Liu, J. Shen, *Appl. Surf. Sci.* **258**, 999 (2011).
27. S. Feng, K. Sato, Y. Kumashiro, *J. Appl. Phys.* **87**, 4031 (2000)
28. T. Yoshitake, T. Nishiyama, H. Aoki, K. Suizu, K. Takahashi, K. Nagayama, *Diamond Relat. Mater.* **8**, 463 (1999).